STEM CELLS AND DEVELOPMENT
Volume 22, Number 6, 2013
© Mary Ann Liebert, Inc.
DOI: 10.1089/scd.2012.0395

Exosomes Derived from Human Umbilical Cord Mesenchymal Stem Cells Alleviate Liver Fibrosis

Tingfen Li,[1,*] Yongmin Yan,[1,*] Bingying Wang,[1] Hui Qian,[1] Xu Zhang,[1] Li Shen,[1] Mei Wang,[1] Ying Zhou,[1] Wei Zhu,[1] Wei Li,[1,2] and Wenrong Xu[1,3]

Mesenchymal stem cells (MSCs) have been considered as an attractive tool for the therapy of diseases. Exosomes excreted from MSCs can reduce myocardial ischemia/reperfusion damage and protect against acute tubular injury. However, whether MSC-derived exosomes can relieve liver fibrosis and its mechanism remain unknown. Previous work showed that human umbilical cord-MSCs (hucMSCs) transplanted into acutely injured and fibrotic livers could restore liver function and improve liver fibrosis. In this study, it was found that transplantation of exosomes derived from hucMSC (hucMSC-Ex) reduced the surface fibrous capsules and got their textures soft, alleviated hepatic inflammation and collagen deposition in carbon tetrachloride (CCl_4)-induced fibrotic liver. hucMSC-Ex also significantly recovered serum aspartate aminotransferase (AST) activity, decreased collagen type I and III, transforming growth factor (TGF)-β1 and phosphorylation Smad2 expression in vivo. In further experiments, we found that epithelial-to-mesenchymal transition (EMT)-associated markers E-cadherin-positive cells increased and N-cadherin- and vimentin-positive cells decreased after hucMSC-Ex transplantation. Furthermore, the human liver cell line HL7702 underwent typical EMT after induction with recombinant human TGF-β1, and then hucMSC-Ex treatment reversed spindle-shaped and EMT-associated markers expression in vitro. Taken together, these results suggest that hucMSC-Ex could ameliorate CCl_4-induced liver fibrosis by inhibiting EMT and protecting hepatocytes. This provides a novel approach for the treatment of fibrotic liver disease.

Introduction

Liver fibrosis is a frequent event in response to a variety of chronic injuries, such as viral hepatitis, alcohol, drugs, metabolic diseases, and autoimmune attack of hepatic cells. It is characterized by excessive extracellular matrix deposition in liver tissue [1–4]. Interstitial fibroblasts are the key mediators of kidney and liver fibrosis, playing a crucial role in the pathogenesis of tissue fibrosis. Several studies have shown that fibroblasts are derived from hepatocytes via epithelial-to-mesenchymal transition (EMT) and produce collagen [5–8]. Major advances have been made in the treatment of liver fibrosis, such as liver transplantation and the use of artificial liver. However, because the number of patients suffering from liver disease is still increasing and there is limited availability of suitable donors, morbidity and mortality from liver fibrosis continue to be an enormous burden experienced by many individuals. Therefore, effective therapies to replace liver transplantation are urgently needed.

The multipotent differentiation ability of mesenchymal stem cells (MSCs) has been reported and it has attracted a lot of attention as a reliable cell source for liver therapy [9–11]. Similar to the MSCs from bone marrow, human umbilical cord-MSCs (hucMSCs) have a high self-renewal ability and low immunogenicity, and hucMSCs can be obtained by a noninvasive procedure and easily cultured, which make them potentially superior to the MSCs from other sources for cell transplantation therapy.

Some people reported that the mechanism of MSCs repaired tissue injury was related to paracrine action rather than transdifferentiation [12–14]. Cell-derived exosomes have been described as a new mechanism of cell-to-cell communication [15]. Exosomes derived MSCs were critical to protect against acute tubular injury [16–18] and reduce myocardial ischemia/reperfusion damage [19], suggesting that exosomes have the ability to serve as a novel therapeutic modality for diseases [20]. So far, our laboratory has reported the potential role of human bone marrow and umbilical cord MSCs in the repair of injured liver and kidney [10,11,21–23]. Then, whether exosomes from MSCs can be exploited following transplantation to reduce liver fibrosis remains largely unknown. In this study, exosomes derived from hucMSC (hucMSC-Ex) were used to treat carbon tetrachloride (CCl_4)-induced mouse liver fibrosis and found that

[1]School of Medical Science and Laboratory Medicine, Jiangsu University, Zhenjiang, Jiangsu, People's Republic of China.
[2]Jiangsu Center for Stem Cell Engineering and Technology, China Medical City, Taizhou, People's Republic of China.
[3]The Affiliated Hospital, Jiangsu University, Zhenjiang, Jiangsu, People's Republic of China.
*These two authors contributed equally to this article.

hucMSC-Ex ameliorated liver injury through inactivating the transforming growth factor (TGF)-β1/Smad signaling pathway and inhibiting the EMT of hepatocytes.

Material and Methods

Isolation of hucMSCs

Fresh umbilical cords were collected from informed, consenting mothers and processed within the optimal period of 6 h as described [24]. Umbilical cords were rinsed twice in phosphate-buffered saline (PBS) containing 5% penicillin and 5% streptomycin until the cord blood was cleared, and cord vessels were removed. Cords were cut into pieces of 1–3 mm^3 and adhered to flasks for 30 min. Cord pieces were then floated in a low-glucose Dulbecco's modified Eagle's medium containing 10% fetal bovine serum (Gibco), 1% penicillin, and 1% streptomycin (Gibco). Cord pieces were subsequently incubated at 37°C in humid air with 5% CO_2. The medium was changed every 3 days after initial plating. When well-developed colonies of fibroblast-like cells reached 80% confluence, cultures were trypsinized with 0.25% trypsin-EDTA (Invitrogen) and passaged into new flasks for further expansion.

Osteogenic and adipogenic differentiation of hucMSCs in vitro

hucMSCs in passage 3 were cultured in a medium that contained either osteogenic (0.1 μM dexamethasone, 10 μM β-glycerophosphate, and 50 μM ascorbate-phosphate) or adipogenic (0.5 μM isobutylmethylxanthine, 1 μM dexamethasone, 10 μM insulin, and 200 μM indomethacin) reagents. All reagents were from Sigma-Aldrich. hucMSCs were cultured in the regular medium as control. Two weeks later, osteogenic differentiation was assessed by the examination of neutrophil alkaline phosphatase (NAP) with the NAP staining kit (Sun Bio) and adipogenic differentiation was examined via intracellular lipid accumulation, which was visualized using Oil-Red-O staining by an inverted microscope (Ti; Nikon Corporation).

Isolation and identification of hucMSC-Ex

hucMSC-Ex were isolated and purified as described previously, with added modifications [25]. Briefly, the conditioned medium was collected and centrifuged at 1,000 *g* for 20 min to remove cell debris, followed by centrifugation at 2,000 *g* for 20 min and 10,000 *g* for 20 min. The supernatant was collected and concentrated using 100 KDa molecular weight cut off (MWCO) (Millipore) at 1,000 *g* for 30 min. The concentrated supernatant was loaded upon 5 mL of 30% sucrose/D_2O cushions, and then ultracentrifuged at 100,000 *g* for 60 min (optimal-90K; Beckman Coulter). The exosome-enriched fraction was diluted with PBS, and then centrifuged thrice at 1,000 *g* for 30 min using 100 KDa MWCO. Finally, the purified exosomes were subjected to filtration on a 0.22-μm pore filter (Millipore) and stored at −80°C. The protein content of the concentrated exosomes was determined using a BCA protein assay kit (Pierce). hucMSCs-Ex were identified by transmission electron microscopy (FEI Tecnai 12; Philips), tetraspan molecules [CD9 (1:500; Bioworld), CD81 (1:1,000; Epitomics)] were verified by western blotting.

CCl_4-induced liver fibrosis and hucMSC-Ex transplantation

Mice (Kunmingbai strains, aged 4–5 weeks) were purchased from the Animal Experimental Center of Jiangsu University. All experimental procedures were in accordance with the Chinese legislation regarding experimental animals. Mice were administered with an intraperitoneal injection of CCl_4 (Nanjing Chemical Company) at a dose of 0.6 mL/kg in vegetable oil, twice in 1 week. Six weeks later, the left and right lobes of mice livers were directly injected with 250 μg hucMSC-Ex in 330 μL PBS (hucMSC-Ex group) ($n = 6$). The control group was administered with PBS alone (PBS group) ($n = 6$). The normal group is without any of treatment. Blood samples were collected every week and the entire liver was taken, fixed, and prepared for further analysis at the end of the experiment.

hucMSC-Ex labeling

hucMSC-Ex were labeled with the crosslinkable membrane dye, CM-Dil, according to the manufacturer's protocol, at a concentration of 1 mL hucMSC-Ex suspension, and then add 5 μL of the CM-Dil cell-labeling solution (CM-Dil; Molecular Probes). Cells were incubated for 30 min at 37°C, then the dye-labeled hucMSC-Ex were transplanted into mouse liver. We used an in vivo imaging system to observe after injection for 4 h.

Quantitative reverse transcription–polymerase chain reaction

Total RNA was extracted with the Trizol reagent according to the manufacturer's instructions (Invitrogen). The cDNA was synthesized using the SuperScript™ II RT kit according to the manufacturer's instructions (Invitrogen). Primers to generate specific products were designed as shown in Table 1. Primers were produced by Shanghai Bio-Engineering Company. Quantitative reverse transcription–polymerase chain reaction (qRT-PCR) was performed using SYBR® qPCR mix (ToYoBo) in a CFX96™ real-time system (Bio Rad). *β-actin* served as an internal control. All reactions were performed in triplicate. Levels are expressed relative to matched control samples from the same time point.

Histopathological staining

Liver tissues were processed for paraffin embedding and were sectioned into 4-μm sections. The sections were stained with hematoxylin and eosin and masson trichrome (MT) according to standard protocols. To analyze the extent of liver fibrosis, randomly picked fields of MT sections were captured from each animal.

Immunohistochemistry

For immunohistochemical staining, the liver slides were incubated with diluted primary antibodies against anti-mouse TGF-β1 (1:200; Bioworld), N-cadherin (1:1,000; BD), E-cadherin, and vimentin (1:50; SAB), according to the manufacturer's instructions. The primary antibody was detected using the biotin-conjugated anti-rabbit immunoglobulin G antibody, and then incubated with streptavidin–biotin. The complex was visualized with the 3,3′-diamino

Table 1. Specific Primers for Target and Control Genes

Target/control gene	*Primer sequence (5′–3′)*	*Annealing temperature (°C)*	*Amplicon size (bp)*
Mouse *TGF-β1*	For: CAAGTGTGGAGCAACATGTG Rev: ATTCCGTCTCCTTGGTTCAG	60	157
Mouse *collagen I*	For: TGAGACAGGCGAACAAGGTG Rev: GCTGAGGCAGGAAGCTGAAG	63	320
Mouse *collagen III*	For: CTGGTCAGCCTGGAGATAAG Rev: ACCAGGACTACCACGTTCAC	58	284
Human *E-cadherin*	For: CGCATTGCCACATACACTCT Rev: TTGGCTGAGGATGGTGTAAG	60	252
Human *N-cadherin*	For: AGTCAACTGCAACCGTGTCT Rev: AGCGTTCCTGTTCCACTCAT	60	337
Human *twist*	For: ACGAGCTGGACTCCAAGATG Rev: GGCACGACCTCTTGAGAATG	60	484
M/H *β-actin*	For: CACGAAACTACCTTCAACTCC Rev: CATACTCCTGCTTGCTGATC	58	265

For, forward; Rev, reverse.

benzidine reagent for microscopic examination. Removal of the primary antibody from the procedure provided a negative control.

Serum assay

The TGF-β1 level in mouse serum was detected by ELISA (Excell). Hyaluronic acid (HA) levels in mouse serum were measured with the double antibody sandwich chemiluminescence method. Serum AST and alanine aminotransferase (ALT) levels were measured with an automated biochemical analyzer.

Western blotting

Liver tissues were harvested, pulverized, and lysed in the RIPA buffer. Equal amounts of protein were loaded and separated on a 12% SDS-PAGE gel. Proteins were transferred to polyvinylidene fluoride membranes (Millipore). After incubation with the primary antibodies overnight at 4°C, membranes were incubated with horse radish peroxidase (HRP)-conjugated goat anti-rabbit, or goat anti-mouse antibodies (1:2,000; Kangcheng). This was followed by detection with a luminata™ crescendo Western HRP substrate (Millipore) and quantitated using a Molecular Dynamics Densitometer (Sage Creation Science) with LANE 1D software. Sources and dilution factors of primary antibodies were mouse polyclonal anti-TGF-β1 (1:500; Bioworld), rabbit polyclonal anti-E-cadherin (1:200; SAB), mouse polyclonal anti-N-cadherin (1:2,000; BD), anti-phosphorylation-Smad2, anti-total-Smad2 (1:500; SAB), and mouse monoclonal anti-GAPDH (1:5,000; Kang Cheng).

Statistical analysis

Data are expressed as means ± standard deviation. Statistical analysis was performed using Prism software (Graph Pad). Analysis of variance was used to analyze variance among all groups, and the Student's *t*-test was performed to compare experimental and relative control groups. Statistical P values < 0.05 were considered significant.

Results

Identification of hucMSCs and hucMSC-Ex

hucMSCs presented a homogeneous population of spindle fibroblast-like cells. They positively expressed CD29, CD44, and HLA-I and negatively expressed CD34, CD38, and HLA-DR by flow cytometry (Fig. 1.A). Numerous lipid droplets were observed with Oil-Red-O staining in hucMSCs after incubation with the adipogenic supplementation for 14 days (Fig. 1.Bb) and positive staining of alkaline phosphatase and Von Kossa were shown after osteogenic induction (Fig. 1.Bd). Control groups did not show any spontaneous adipocyte or osteoblast formation (Fig. 1.Ba, c). By transmission electron microscope, it was found that hucMSC-Ex were 40–100 nm microvesicles (MVs) (Fig. 1Ca). hucMSC-Ex showed the positive expression of exosomal markers, such as CD9 and CD81 (Fig. 1Cb).

hucMSC-Ex location in mouse liver

The cell dye-labeled hucMSC-Ex were administered into mouse liver for 4 h, an in vivo imaging system was used to find the PBS group liver had no fluorescence (Fig. 2Aa) and hucMSC-Ex treatment had red fluorescence in 90% of the liver (Fig. 2Ab). This data illustrated that hucMSC-Ex located to the liver.

hucMSC-Ex alleviated CCl_4-induced mouse liver fibrosis

The normal mouse liver had a smooth surface, uniform and soft textures (Fig. 2Ba). Six weeks after CCl_4 administration, the surface of the mice livers had fibrous capsules and their textures turned hard (Fig. 2Bb). Three weeks after transplantation, hucMSC-Ex group livers (Fig. 2Bd) were softer than the PBS group (Fig. 2Bc).

Mice livers of PBS groups had apparent fibrosis conformation (Fig. 2Cb–d), which the normal liver had not (Fig. 2Ca). The recovery of injured livers was continuously investigated for 3 weeks after hucMSC-Ex treatment. At 1 week, injured livers between PBS (Fig. 2Cb) and hucMSC-Ex groups (Fig. 2Ce) had no difference, with visible fibrosis, destruction of hepatic lobules, a large amount of hepatocyte apoptosis, and infiltration of inflammatory cells. However, at 2 weeks, hucMSC-Ex treatment inhibited hepatocyte apoptosis and hepatic lobule destruction; PBS treatment did not (Fig. 2Cf, c). Interestingly, 3 weeks after hucMSC-Ex treatment, CCl_4-induced liver fibrosis was significantly alleviated (compare Fig. 2Cg with Fig. 2Cd).

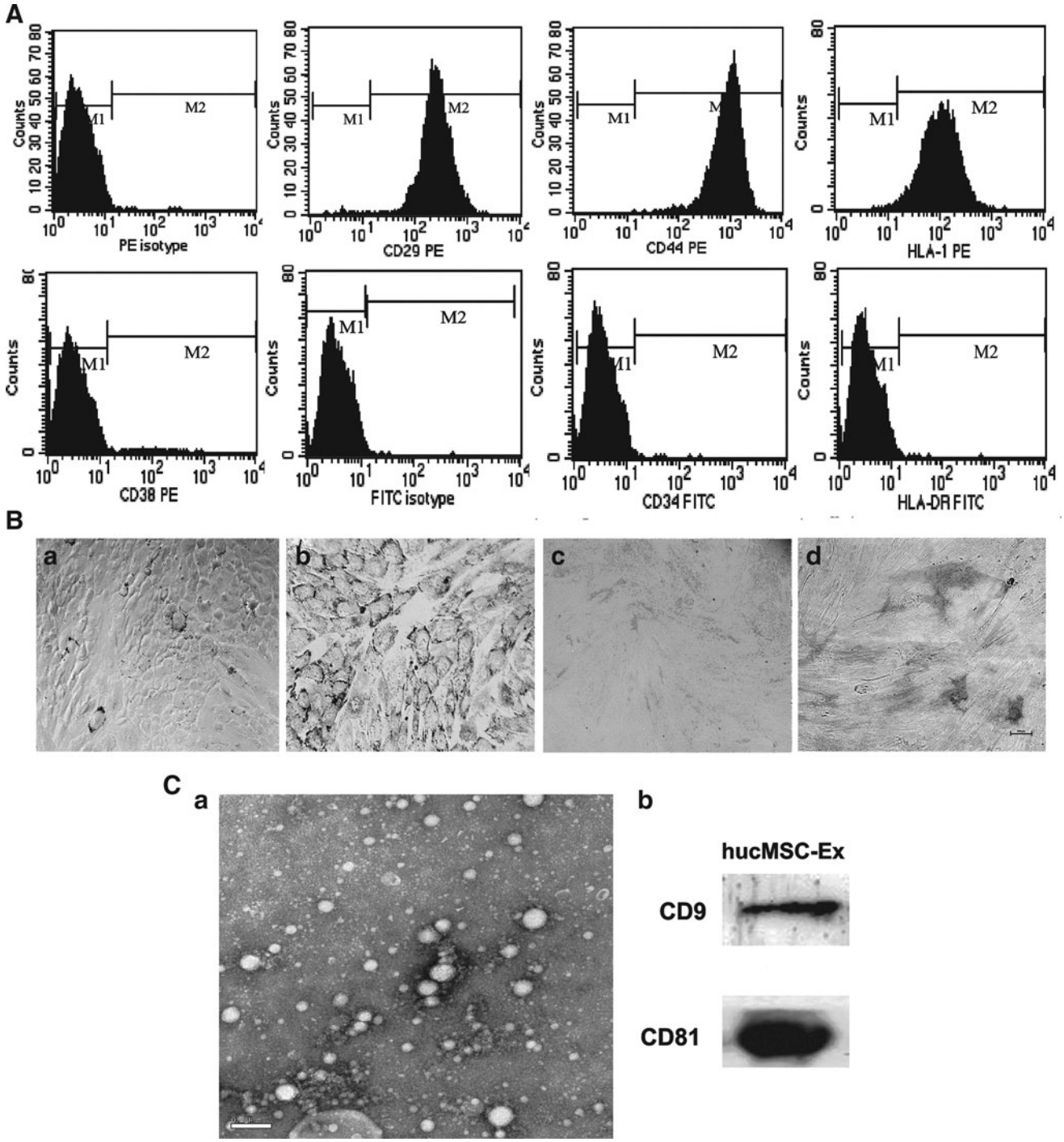

FIG. 1. Identification of human umbilical cord-mesenchymal stem cells (hucMSCs) and exosomes derived from hucMSC (hucMSC-Ex). **(A)** Flow cytometry analysis of the surface markers in hucMSCs. **(B)** Adipogenic and osteogenic differentiation of hucMSCs (100×). **(a, b)** Results of Oil-Red-O staining detection in hucMSCs cultures grown for 14 days; **(a)** hucMSCs cultured in the regular medium; **(b)** hucMSCs cultured in adipogenic medium; **(c, d)** Results of neutrophil alkaline phosphatase (NAP) with NAP staining kit detection in hucMSCs cultures grown for 14 days; **(c)** hucMSCs cultured in the regular medium; **(d)** hucMSCs cultured in osteogenic medium. **(C)** Identification of hucMSCs-Ex. **(a)** Transmission electron micrograph of hucMSC-Ex, Scale bar = 200 nm; **(b)** Detection of hucMSC-Ex CD9 and CD81 expression by western blotting.

The level of serum HA is a sign of liver fibrosis [26]. Comparing to the normal group, it was found that serum HA levels of the PBS group increased remarkably. Meanwhile, hucMSC-Ex transplantation decreased serum HA levels compared to the PBS group (Fig. 2D). Also serum TGF-β1 levels declined after hucMSC-Ex treatment as assayed by ELISA; PBS treatment did not decrease the TGF-β1 content (Fig. 2E). After CCl_4 injury for 9 weeks, the serum AST level increased obviously in the PBS group, while hucMSC-Ex transplantation almost kept AST at normal levels. There was no difference in the Serum ALT level between hucMSC-Ex and PBS groups (Fig. 2F).

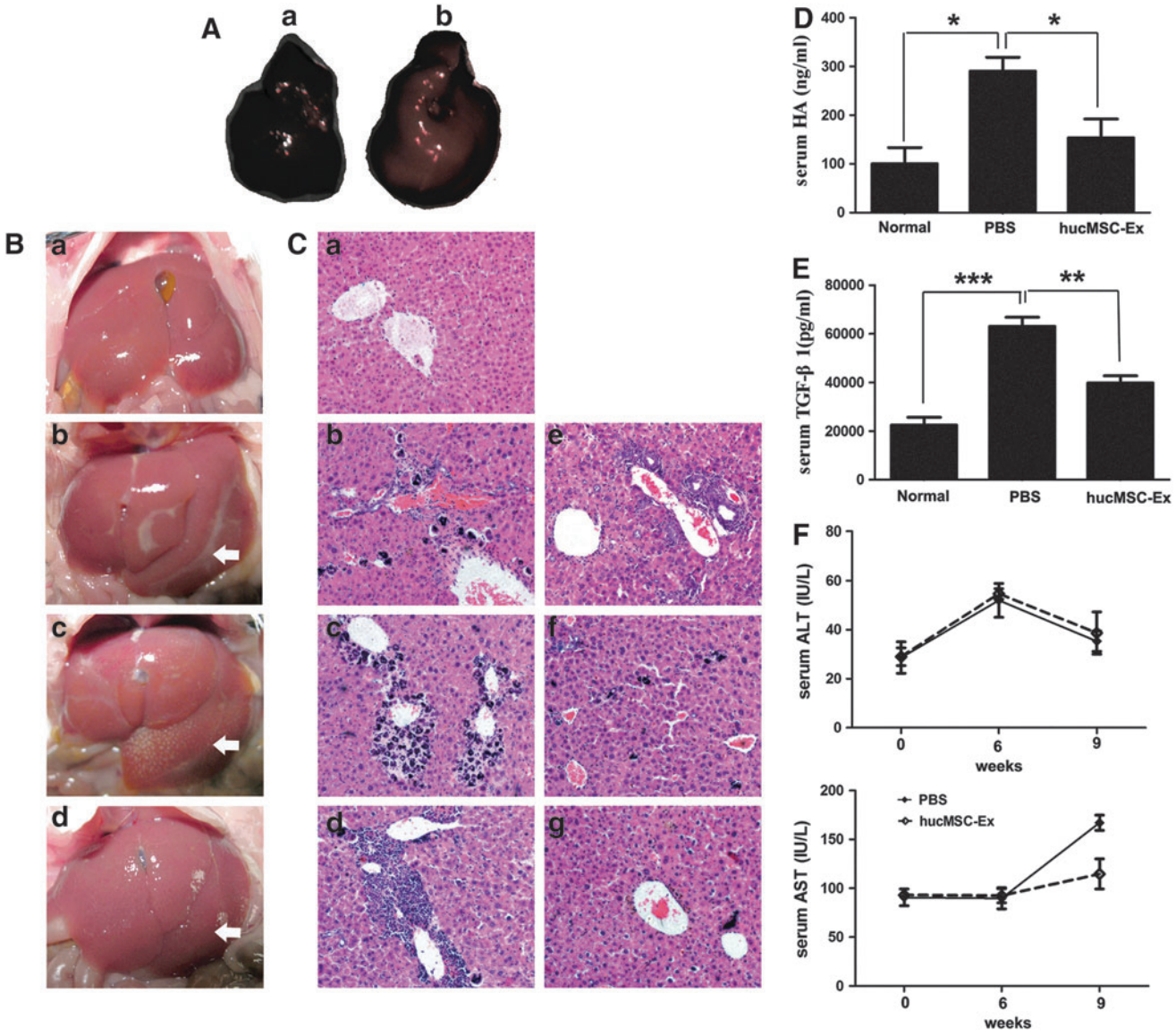

FIG. 2. hucMSC-Ex promoted the recovery of carbon tetrachloride (CCl_4)-induced mouse liver injury. **(A)** hucMSC-Ex location in mouse liver by an in vivo imaging system. **(a)** The phosphate-buffered saline (PBS) group liver; **(b)** The cell dye-labeled hucMSC-Ex administrated into mouse liver showed *red* fluorescence. **(B)** Pictures of mouse livers. **(a)** normal group; **(b)** CCl_4 group, 6 weeks after CCl_4 injury; **(c)** PBS group 3 weeks after PBS treatment; **(d)** hucMSCs-Ex group 3 weeks after hucMSC-Ex transplantation. The *arrows* indicated the liver damage/fibrotic areas. **(C)** Hematoxylin and eosin dyeing of liver sections (200×). **(a)** normal group; **(b)** PBS group, 1 week; **(c)** PBS group, 2 weeks; **(d)** PBS group, 3 weeks; **(e)** hucMSC-Ex group, 1 week; **(f)** hucMSC-Ex group, 2 weeks; **(g)** hucMSC-Ex group, 3 weeks. **(D)** Serum hyaluronic acid (HA) level 3 weeks after hucMSC-Ex transplantation. **(E)** Serum transforming growth factor (TGF)-β1 level 3 weeks after hucMSC-Ex transplantation. **(F)** Serum alanine aminotransferase (ALT) and aspartate aminotransferase (AST) levels after hucMSC-Ex transplantation. *$P < 0.05$, **$P < 0.01$, and ***$P < 0.001$.

hucMSC-Ex reduced the expression of collagen I and III

Blue/green matrixes indicated collagen deposition in tissue sections with MT dyeing. Much of the collagen deposition was observed in the PBS group livers (Fig. 3Ab–d); the normal liver did not have any collagen deposition (Fig. 3Aa). One week after hucMSC-Ex transplantation, collagen did not decline (Fig. 3Ae). However, after 2 weeks, collagen started to decrease (Fig. 3Af) and it reduced remarkably after 3 weeks (Fig. 3Ag). Quantitative RT-PCR showed that the expression of *collagen I* and *III* mRNAs in PBS livers increased, and *collagen I* and *III* mRNA expression decreased significantly after 3 weeks from hucMSC-Ex transplantation ($P < 0.05$) (Fig. 3B).

hucMSC-Ex inactivated the TGF-β1/Smad signaling pathway

The TGF-β1/Smad pathway is greatly associated with liver fibrosis. Three weeks after CCl_4 treatment, TGF-β1 expression was detected in liver. Quantitative RT-PCR showed

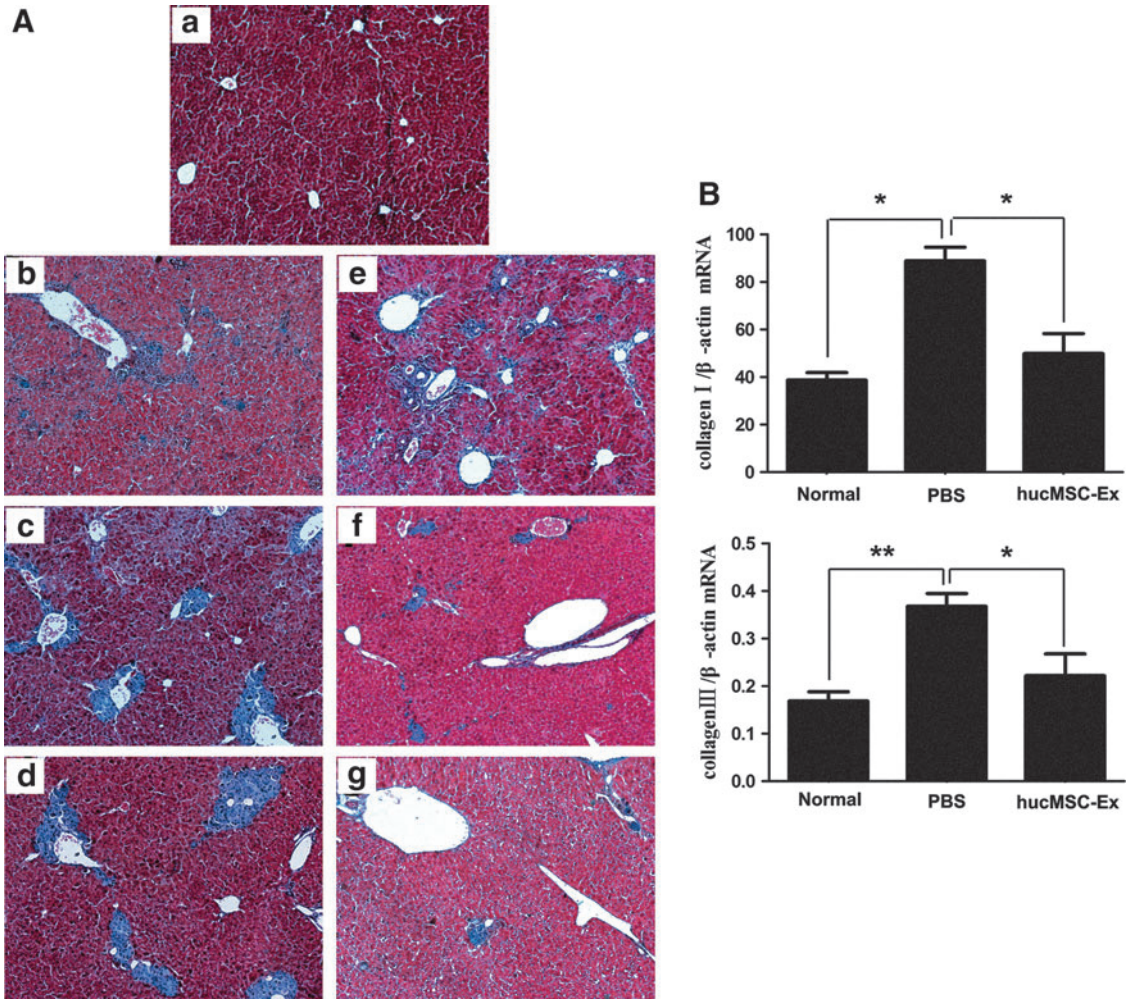

FIG. 3. hucMSC-Ex reduced collagen deposition and inhibited the expression of collagen mRNA. **(A)** Masson's trichrome stain of liver sections (100×). **(a)** normal group; **(b)** PBS group, 1 week; **(c)** PBS group, 2 weeks; **(d)** PBS group, 3 weeks; **(e)** hucMSC-Ex group, 1 week; **(f)** hucMSC-Ex group, 2 weeks; **(g)** hucMSC-Ex group, 3 weeks. **(B)** Quantitative analyses of type I and III *collagen* mRNA expression 3 weeks after hucMSC-Ex transplantation. *$P < 0.05$ and **$P < 0.01$.

that the expression of *TGF-β1* mRNA was increased in the PBS group ($P < 0.01$); it declined significantly in the hucMSC-Ex group compared with the PBS group ($P < 0.05$) (Fig. 4A). A similar result of TGF-β1 was confirmed by western blotting (Fig. 4B). TGF-β1-positive cells in the hucMSC-Ex group were less than that in the PBS group by immunohistochemistry (Fig. 4C).

TGF-β1/Smad pathway activation is critical to EMT. The effect of hucMSC-Ex on the status of Smad was investigated and it was found that the phosphorylation of Smad2 increased in the PBS group; it decreased significantly after hucMSC-Ex transplantation (Fig. 4B).

hucMSC-Ex inhibited EMT

EMT is a physiological process in liver fibrosis. Three weeks after hucMSC-Ex transplantation, immunohistochemistry results showed E-cadherin-positive cells in liver (Fig. 5Ac) were more than the PBS group (Fig. 5Ab), as well as the normal liver (Fig. 5Aa). Meanwhile, N-cadherin- and vimentin-positive cells in the hucMSC-Ex group (Fig. 5Af, i) were less than that in the PBS group (Fig. 5Ae, h).

hucMSC-Ex reserved TGF-β1-induced EMT in HL7702 cell line in vitro

Typically, the human epithelioid liver cell line, HL7702, turns to fibroblasts with recombinant human TGF-β1 treatment for 3 days (Fig. 6Ab). Then, the hucMSC-Ex (100 μg/mL) treatment for 3 days reversed the morphology switch (Fig. 6Ad); without hucMSCs-Ex treatment, there was no change (Fig. 6Ac). After TGF-β1 induction for 3 days, the expression of *E-cadherin* mRNA decreased, while *N-cadherin* and *Twist* mRNA expression increased in HL7702 cells by quantitative RT-PCR. However, after hucMSC-Ex treatment for 3 additional days, *E-cadherin* mRNA expression increased and *N-cadherin* and *Twist* mRNA expressions decreased (Fig. 6B). There were similar results for N-cadherin and E-cadherin by western blotting (Fig. 6C).

Discussion

MSCs are a promising therapeutic tool for diseases, such as liver failure, kidney injury, and myasthenia gravis. In recent years, hucMSCs represent a novel source of MSCs for

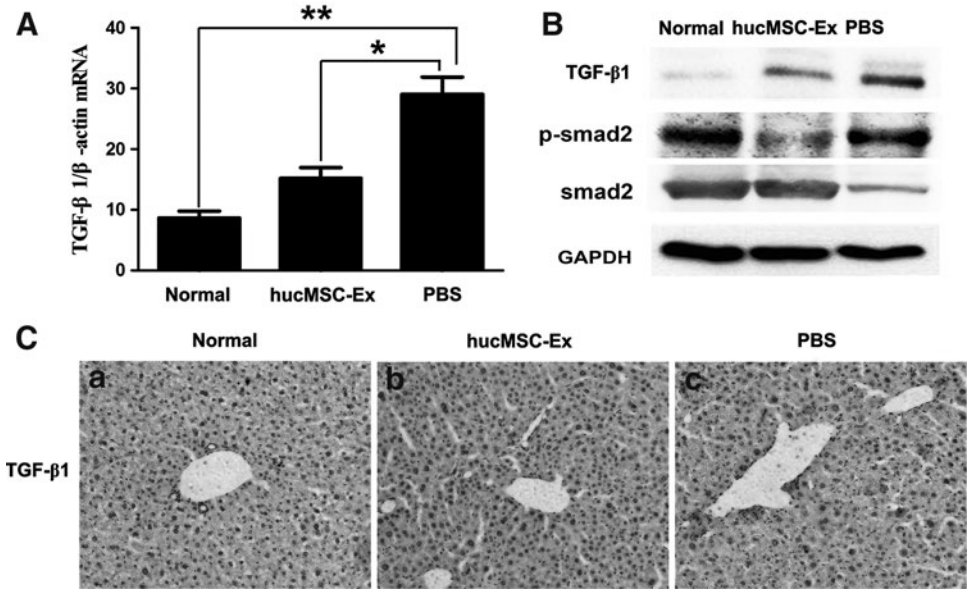

FIG. 4. hucMSC-Ex inactivated TGF-β1/Smad signaling pathway. **(A)** Quantitative reverse transcription–polymerase chain reaction (qRT-PCR) analyses of *TGF-β1* expression 3 weeks after hucMSC-Ex transplantation. **(B)** Western blotting analysis of TGF-β1 and Smad2 expression 3 weeks after hucMSC-Ex transplantation. **(C)** Immunohistochemical analysis of TGF-β1 expression 3 weeks after hucMSC-Ex transplantation (200×). **(a)** normal group; **(b)** hucMSC-Ex group; **(c)** PBS group. $^{*}P < 0.05$ and $^{**}P < 0.01$.

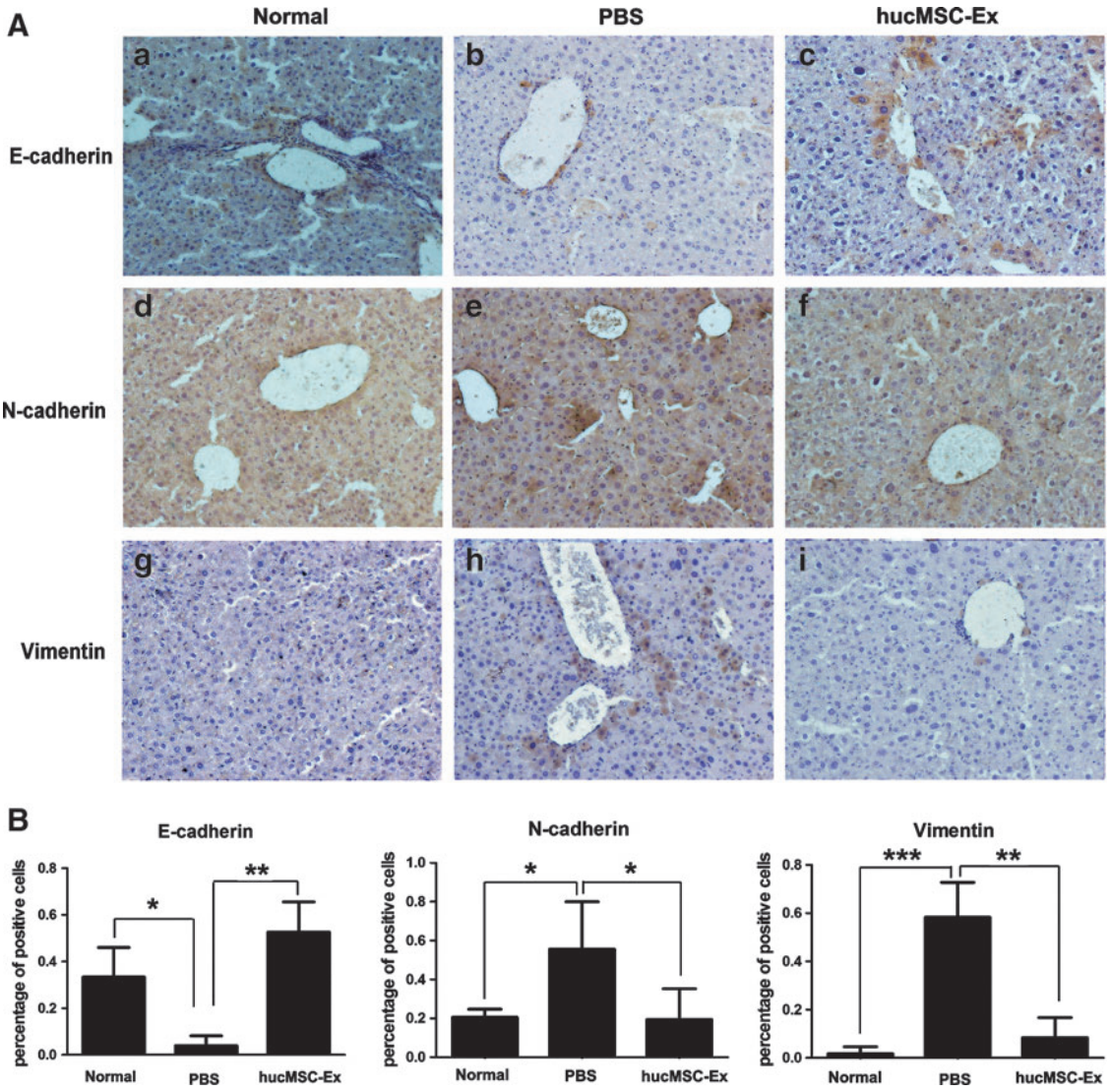

FIG. 5. hucMSC-Ex inhibited epithelial-to-mesenchymal transition (EMT). **(A)** Immunohistochemistry analysis of E-cadherin, N-cadherin, and vimentin 3 weeks after hucMSC-Ex transplantation (200×). **(a, d, g)** normal group; **(b, e, h)** PBS group; **(c, f, i)** hucMSC-Ex group. **(B)** Positive cells analysis of immunohistochemical sections. ($n = 3$). $^{*}P < 0.05$, $^{**}P < 0.01$, and $^{***}P < 0.001$.

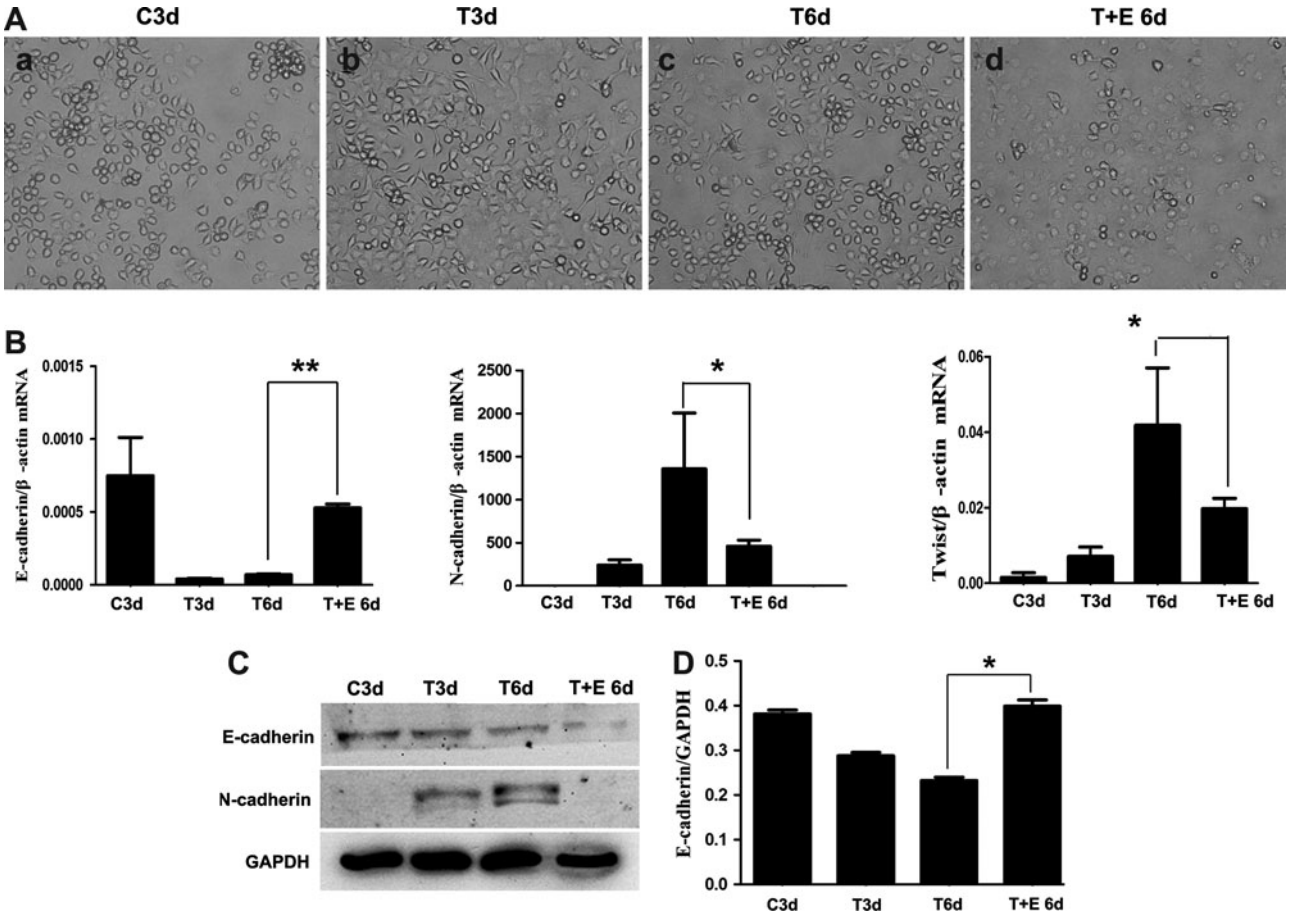

FIG. 6. hucMSC-Ex reversed TGF-β1-induced EMT in human hepatocyte cell line HL7702 cells. **(A)** The morphology of HL7702 cells treated with TGF-β1 for 3 days followed by hucMSC-Ex for 3 days (200×). **(a)** HL7702 cells, 3 days (C3d); **(b)** TGF-β1 + HL7702, 3 days (T3d); **(c)** TGF-β1 + HL7702, 6 days (T6d); **(d)** TGF-β1 + HL7702 + hucMSC-Ex, 6 days (T + E 6d). **(B)** Quantitative RT-PCR analyses of *E-cadherin*, *N-cadherin*, and *Twist* mRNA expression. **(C)** Western blotting analyses of E-cadherin and N-cadherin expression in cells. **(D)** Density analysis of western blot bands. $^{*}P < 0.05$ and $^{**}P < 0.01$.

tissue injury because there are no ethical considerations. Work by Zhang et al. [27] suggest that hucMSCs significantly improve liver function and reduce ascites in decompensated liver cirrhosis patients. Tsai et al. [28] reported that hucMSCs alleviated the rat liver fibrosis and reduced collagen deposition. Further work shows that the mechanism was by secreting a variety of bioactive cytokines, but not differentiating into hepatocytes. Zhang et al. [29] compared hucMSCs with adult human hepatocyte (AHH) transplantation and found that hucMSCs transplantation was more effective than AHH treatment and successfully decreased systemic inflammatory cytokines. Furthermore, hucMSCs cocultured with CCl_4-damaged mouse hepatocytes (MHs) were compared with AHH in vitro. The author identified that hucMSCs enhanced the regeneration of MHs by producing paracrine effects. Our previous work showed that hucMSCs reduced α-smooth muscle actin, fibroblast-specific protein-1, decreased ALT and AST, enhanced recovery of CCl_4-injured mouse liver [10].

Some articles revealed that MSCs might perform their therapeutic roles through paracrine mechanism [12–14,30]. Bruno et al. reported that some mRNAs and surface molecules of human bone marrow MSC-derived MVs, were critical to protect against acute tubular injury [16–18] and myocardial ischemia/reperfusion damage [19]. Work by Herrera et al. shows that human stem cell-derived exosomes accelerate hepatic regeneration in hepatectomized rats. Further work confirmed that some mRNAs and adhesion molecules of exosomes play a critical role [31]. Furthermore, the MSC has an effect on immunomodulatory properties [32]. MSC-derived MVs (exosomes) are viewed as potential mediators for induction of peripheral tolerance and modulation of immune responses [33]. Bruno et al. and Gatti et al. also found that human-derived exosomes can be successfully used in kidney injury and enhance survival in mice model [16–18]. In this study, exosomes derived from humans were used in mice and no evidence of immune rejection was found during the transplantation in mice. The isolation of exosomes from hucMSCs was successful, confirming their diameters at about 40–100 nm and protein expression of CD9 and CD81. Further experiment found that hucMSC-Ex transplanted into mouse liver fibrosis, also successfully downregulated serum fibrotic marker HA and TGF-β1, decreased the serum AST level, and reduced hepatic inflammation and collagen deposition in the liver fibrosis, and enhanced the recovery of hepatocyte damage.

Accumulating evidence has demonstrated the repair role of human bone marrow or umbilical cord MSCs in liver fibrosis, but the specific mechanism is still not clear. Some studies have reported that upon phosphorylation, Smad2 and Smad3 form complexes with Smad4 and, subsequently, translocate into the nucleus to regulate the transcription of target genes responsible for EMT, such as Smad7, snail, and collagen type I [8,34,35]. Our work mainly investigated how hucMSC-Ex recovered the liver fibrosis, focusing on the regulation of the TGF-β1/Smad signaling pathway inactivation and EMT inhibition. Six weeks after CCl_4-induced liver fibrosis, it was found that TGF-β1 levels in serum and liver increased. Several studies reported that TGF-β1 activated the Smad2/3 pathway in hepatocytes and induced EMT [7,8]. In this study, it was confirmed that TGF-β1 activated the phosphorylation of Smad2 and led to liver EMT in vivo. Furthermore, the human liver cell line, HL7702, underwent typical EMT with recombinant human TGF-β1 induction for 3 days in vitro. However, it was found that hucMSC-Ex transplantation reduced TGF-β1 expression, inactivated the phosphorylation of Smad2, and reversed liver EMT in vivo. After HL7702 cells happened to EMT, hucMSC-Ex treatment reversed spindle-shaped cells and EMT-associated marker expression in vitro.

In conclusion, these findings suggest that hucMSC-Ex inhibit EMT and ameliorate CCl_4-induced liver fibrosis. The study provided a novel mechanism for MSC-mediated tissue repair and an alternative source for the treatment of fibrotic liver disease. Whether or not the mRNA of hucMSC-Ex and its surface adhesion molecules play a critical role in inhibiting EMT and treatment of liver fibrosis needs to be further investigated.

Acknowledgment

This work was supported by the Major Research Plan of the National Natural Science Foundation of China (grant no. 91129718), the National Natural Science Foundation of China (grant nos. 81200312, 31140063, 81272481, and 81000181), Jiangsu Province's Scientific and Technological Supporting Program (grant no. BE2010703), the Natural Science Foundation for Young Scholars of Jiangsu Province (grant no. BK2012288), the Scientific Research Foundation of Jiangsu University (grant nos. 07JDG056 and 11JDG062), and the Sci-tech Innovation Team and Talents of Jiangsu University (grant no. 2008-018-02).

Author Disclosure Statement

No competing financial interests exist.

References

1. Snowdon VK and JA Fallowfield. (2011). Models and mechanisms of fibrosis resolution. Alcohol Clin Exp Res 35:794–799.
2. Ghatak S, A Biswas, GK Dhali, A Chowdhury, JL Boyer and A Santra. (2011). Oxidative stress and hepatic stellate cell activation are key events in arsenic induced liver fibrosis in mice. Toxicol Appl Pharmacol 251:59–69.
3. Domitrović R and H Jakovac. (2011). Effects of standardized bilberry fruit extract on resolution of CCl4-induced liver fibrosis in mice. Food Chem Toxicol 49:848–854.
4. Malhi H and GJ Gores. (2008). Cellular and molecular mechanisms of liver injury. Gastroenterology 134:1641–1654.
5. Zeisberg M, C Yang, M Martino, MB Duncan, F Rieder, H Tanjore and R Kalluri. (2007). Fibroblasts derive from hepatocytes in liver fibrosis via epithelial to mesenchymal transition. J Biol Chem 282:23337–23347.
6. Iwano M, D Plieth, TM Danoff, C Xue, H Okada and EG Neilson. (2002). Evidence that fibroblasts derive from epithelium during tissue fibrosis. J Clin Invest 110:341–350.
7. Chen YL, J Lv, XL Ye, MY Sun, Q Xu, CH Liu, LH Min, HP Li, P Liu and X Ding. (2011). Sorafenib inhibits tansforming growth factor β1-mediated epithelial-mesenchymal transition and apoptosis in mouse hepatocytes. Hepatology 53: 1708–1718.
8. Kaimori A, J Potter, JY Kaimori, C Wang, E Mezey and A Koteish. (2007). Transforming growth factor-beta1 induces an epithelial-to-mesenchymal transition state in mouse hepatocytes in vitro. J Biol Chem 282:22089–22101.
9. Kanazawa H, Y Fujimoto, T Teratani, J Iwasaki, N Kasahara, K Negishi, T Tsuruyama, S Uemoto and EY Kobayashi. (2011). Bone marrow-derived mesenchymal stem cells ameliorate hepatic ischemia reperfusion injury in a rat model. PLoS One 6:e19195.
10. Yan Y, W Xu, H Qian, Y Si, W Zhu, H Cao, H Zhou and F Mao. (2009). Mesenchymal stem cells from human umbilical cords ameliorate mouse hepatic injury in vivo. Liver Int 29:356–365.
11. Xu H, H Qian, W Zhu, X Zhang, Y Yan, F Mao, M Wang, H Xu and W Xu. (2012). Mesenchymal stem cells relieve fibrosis of Schistosoma japonicum-induced mouse liver injury. Exp Biol Med (Maywood) 237:585–592.
12. Tögel F, K Weiss, Y Yang, Z Hu, P Zhang and C Westenfelder. (2007). Vasculotropic, paracrine actions of infused mesenchymal stem cells are important to the recovery from acute kidney injury. Am J Physiol Renal Physiol 292:F1626–F1635.
13. Camussi G, MC Deregibus and C Tetta. (2010). Paracrine/endocrine mechanism of stem cells on kidney repair: role of microvesicle-mediated transfer of genetic information. Curr Opin Nephrol Hypertens 19:7–12.
14. Qin ZH, JF Xu, JM Qu, J Zhang, Y Sai, CM Chen, L Wu and L Yu. (2012). Intrapleural delivery of MSCs attenuates acute lung injury by paracrine/endocrine mechanism. J Cell Mol Med [Epub ahead of print]; DOI: 10.1111/j.1582-4934.2012.01597.x.
15. Schorey JS and S Bhatnagar. (2008). Exosome function: from tumor immunology to pathogen biology. Traffic 9:871–881.
16. Bruno S, C Grange, MC Deregibus, RA Calogero, S Saviozzi, F Collino, L Morando, A Busca, M Falda, et al. (2009). Mesenchymal stem cell-derived microvesicles protect against acute tubular injury. J Am Soc Nephrol 20:1053–1067.
17. Gatti S, S Bruno, MC Deregibus, A Sordi, V Cantaluppi, C Tetta and G Camussi. (2011). Microvesicles derived from human adult mesenchymal stem cells protect against ischaemia-reperfusion-induced acute and chronic kidney injury. Nephrol Dial Transplant 26:1474–1483.
18. Bruno S, C Grange, F Collino, MC Deregibus, V Cantaluppi, L Biancone, C Tetta and G Camussi. (2012). Microvesicles derived from mesenchymal stem cells enhance survival in a lethal model of acute kidney injury. PLoS One 7:e33115.
19. Lai RC, F Arslan, MM Lee, NS Sze, A Choo, TS Chen, M Salto-Tellez, L Timmers, CN Lee, et al. (2010). Exosome secreted by MSC reduces myocardial ischemia/reperfusion injury. Stem Cell Res 4:214–222.

20. Lai RC, TS Chen and SK Lim. (2011). Mesenchymal stem cell exosome: a novel stem cell-based therapy for cardiovascular disease. Regen Med 6:481–492.
21. Qian H, H Yang, W Xu, Y Yan, Q Chen, W Zhu, H Cao, Q Yin, H Zhou, F Mao and Y Chen. (2008). Bone marrow mesenchymal stem cells ameliorate rat acute renal failure by differentiation into renal tubular epithelial-like cells. Int J Mol Med 22:325–332.
22. Chen Y, H Qian, W Zhu, X Zhang, Y Yan, S Ye, X Peng, W Li and W Xu. (2011). Hepatocyte growth factor modification promotes the amelioration effects of human umbilical cord mesenchymal stem cells on rat acute kidney injury. Stem Cell Dev 20:103–113.
23. Cao H, H Qian, W Xu, W Zhu, X Zhang, Y Chen, M Wang, Y Yan and Y Xie. (2010). Mesenchymal stem cells derived from human umbilical cord ameliorate ischemia/reperfusion-induced acute renal failure in rats. Biotechnol Lett 32:725–732.
24. Qiao C, W Xu, W Zhu, J Hu, H Qian, Q Yin, R Jiang, Y Yan, F Mao, et al. (2008). Human mesenchymal stem cells isolated from the umbilical cord. Cell Biol Int 32:8–15.
25. Zhu W, L Huang, Y Li, X Zhang, J Gu, Y Yan, X Xu, M Wang, H Qian and W Xu. (2012). Exosomes derived from human bone marrow mesenchymal stem cells promote tumor growth in vivo. Cancer Lett 315:28–37.
26. Li F, CL Zhu, H Zhang, H Huang, Q Wei, X Zhu and XY Cheng. (2012). Role of hyaluronic acid and laminin as serum markers for predicting significant fibrosis in patients with chronic hepatitis B. Braz J Infect Dis 16:9–14.
27. Zhang Z, H Lin, M Shi, R Xu, J Fu, J Lv, L Chen, S Lv, Y Li, et al. (2012). Human umbilical cord mesenchymal stem cells improve liver function and ascites in decompensated liver cirrhosis patients. J Gastroenterol Hepatol 2:112–120.
28. Tsai PC, TW Fu, YM Chen, TL Ko, TH Chen, YH Shih, SC Hung and YS Fu. (2009). The therapeutic potential of human umbilical mesenchymal stem cells from Wharton's jelly in the treatment of rat liver fibrosis. Liver Transpl 15:484–495.
29. Zhang S, L Chen, T Liu, B Zhang, D Xiang, ZG Wang and Y Wang. (2012). Human umbilical cord matrix stem cells efficiently rescue acute liver failure through paracrine effects rather than hepatic differentiation. Tissue Eng Part A 18: 1352–1364.
30. Meirelles Lda S, AM Fontes, DT Covas and AI Caplan. (2009). Mechanisms involved in the therapeutic properties of mesenchymal stem cells. Cytokine Growth Factor Rev 20:419–427.
31. Herrera MB, V Fonsato, S Gatti, MC Deregibus, A Sordi, D Cantarella, R Calogero, B Bussolati, C Tetta and G Camussi. (2010). Human liver stem cell-derived microvesicles accelerate hepatic regeneration in hepatectomized rats. J Cell Mol Med 14:1605–1618.
32. Franquesa M, MJ Hoogduijn, O Bestard and JM Grinyó. (2012). Immunomodulatory effect of mesenchymal stem cells on B cells. Front Immunol 3:212.
33. Mokarizadeh A, N Delirezh, A Morshedi, G Mosayebi, AA Farshid and K Mardani. (2012). Microvesicles derived from mesenchymal stem cells: potent organelles for induction of tolerogenic signaling. Immunol Lett 147:47–54.
34. Massagué J and YG Chen. (2000). Controlling TGF-beta signaling. Genes Dev 14:627–644.
35. Cho HJ, KE Baek, S Saika, MJ Jeong and J Yoo. (2007). Snail is required for transforming growth factor-beta-induced epithelial-mesenchymal transition by activating PI3 kinase/Akt signal pathway. Biochem Biophys Res Commun 353: 337–343.

Address correspondence to:
Prof. Hui Qian
School of Medical Science and Laboratory Medicine
Jiangsu University
301 Xuefu Road
Zhenjiang
Jiangsu 212013
People's Republic of China

E-mail: lstmmmlst@163.com

Prof. Wenrong Xu
The Affiliated Hospital
Jiangsu University
228 Jiefang Road
Zhenjiang
Jiangsu 212001
People's Republic of China

E-mail: icls@ujs.edu.cn

Received for publication July 23, 2012
Accepted after revision September 23, 2012
Prepublished on Liebert Instant Online September 24, 2012